

## Nanofibers of Conjugated Polymers Prepared by Electrospinning with a Two-Capillary Spinneret\*\*

By Dan Li, Amit Babel, Samson A. Jenekhe, and Younan Xia\*

Electrospinning has attracted rapidly increasing attention as a simple method for generating nanofibers made of polymers, ceramics, and composites.<sup>[1,2]</sup> Nonwoven mats of nanofibers have found applications in areas such as tissue engineering,<sup>[3]</sup> catalysis,<sup>[4]</sup> and sensing,<sup>[5]</sup> and in fabrication of composite materials,<sup>[6]</sup> supercapacitors,<sup>[7]</sup> and lithium-ion batteries.<sup>[8]</sup> Recent demonstrations have also established that it is convenient to fabricate electrospun nanofibers as uniaxially aligned arrays and to manipulate individual nanofibers by modifying the designs of collectors.<sup>[9]</sup> As a nonmechanical fiber-drawing method, electrospinning involves the stretching of a polymer solution (or melt) with electrostatic forces.<sup>[10]</sup> Successful electrospinning requires the use of an appropriate solvent and polymer system to prepare solutions exhibiting the desired viscoelastic behavior. The traditional setup for electrospinning works well for most conventional polymers, but it cannot be easily applied to polymers with limited solubilities (e.g., conjugated polymers) or low molecular weights. Conjugated polymers are important for their unique combination of electronic, optical, and mechanical properties.<sup>[11]</sup> Nanowires or nanofibers made of conjugated polymers present an ideal system for studying charge transport and luminescence in one-dimensional (1D) systems, and hold promise as the building blocks for nanoelectronics. Moreover, previous studies have shown that the strong stretching forces associated with electrospinning may induce orientation of polymer chains along the long axis of a fiber.<sup>[12]</sup> It is expected that such aligned nanofibers of conjugated polymers may exhibit unique properties such as high charge-carrier mobility or polarized photoluminescence.<sup>[13]</sup> As a result, it is highly desirable to apply electrospinning to the fabrication of nanofibers from this particular class of functional polymers.

As described in the literature, one of the most effective strategies for improving the spinnability of conjugated poly-

mers is to blend these polymers with other spinnable polymers in solution. This method requires the availability of a common solvent that is capable of dissolving both blend components. Furthermore, the solvent must be suitable for electrospinning. Because it is not easy to meet both of these criteria simultaneously, only a few conjugated polymers (e.g., polyaniline and polythiophene) have been prepared as nanofibers by electrospinning.<sup>[14]</sup> We, and other groups, have recently developed a spinneret consisting of two coaxial capillaries that can be used to directly electrospin or electrospray two different liquids into a compound jet. Core-sheath and hollow fibers, and core-shell particles, have been successfully prepared using this setup.<sup>[15]</sup> Here we demonstrate that the capability of this new setup could be further extended to directly electrospin conjugated polymers into uniform nanofibers with controllable diameters and morphologies.

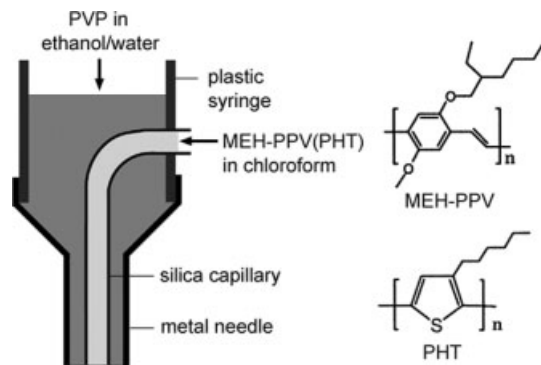
We selected poly[2-methoxy-5-(2-ethylhexyloxy)-1,4-phenylenevinylene] (MEH-PPV) as an example for demonstrating the concept. MEH-PPV has been widely studied for its excellent luminescent properties and device applications in light-emitting diodes,<sup>[16a]</sup> solar cells,<sup>[16b-d]</sup> and optically pumped lasers.<sup>[16e]</sup> MEH-PPV nanostructures have been fabricated by electron-beam lithography and dip-pen nanolithography, albeit the productivity of these serial techniques is relatively low.<sup>[17]</sup> Recently, Balkus and coworkers demonstrated that MEH-PPV could be electrospun as fibers with a mean diameter around 200 nm by dissolving the polymer in 1,2-dichloroethane.<sup>[18]</sup> However, a large amount of large, leaf-like structures also coexisted in the final products. Although the fraction of such leaf-like structures could be reduced by co-spinning the MEH-PPV solution with a silica sol using a side-by-side dual-syringe system, the mean diameter of the resultant composite fibers increased to 700–800 nm.<sup>[18]</sup> We have attempted to prepare high-quality MEH-PPV nanofibers by co-dissolving this polymer with poly(vinyl pyrrolidone) (PVP) in chloroform, but failed because chloroform is not a suitable solvent for electrospinning PVP. Our previous work showed that uniform PVP nanofibers could be readily electrospun from an ethanol/water mixture and could serve as the matrix to host inorganic precursors for preparing ceramic nanofibers.<sup>[9a,19]</sup> Unfortunately, MEH-PPV is insoluble in this solvent mixture, and MEH-PPV immediately precipitated when a MEH-PPV solution in chloroform was poured into a PVP solution in the ethanol/water mixture. Although these two solutions are not compatible in the conventional mixing process, here we demonstrate that they could be co-electrospun through a two-capillary spinneret to generate uniform nanofibers with homogeneously blended compositions.

Scheme 1 shows a schematic of the spinneret design we used for electrospinning. It can be easily fabricated in any research laboratory by inserting a polymer-coated silica capillary into a stainless-steel needle.<sup>[15a]</sup> In a typical electrospinning procedure, a PVP solution in the ethanol/water mixture and a MEH-PPV solution in chloroform were simultaneously fed through the outer and inner capillaries, respectively. The feed rates of both solutions could be precisely controlled

[\*] Prof. Y. Xia, Dr. D. Li  
Department of Chemistry  
University of Washington  
Seattle, WA 98195 (USA)  
E-mail: xia@chem.washington.edu

A. Babel, Prof. S. A. Jenekhe  
Departments of Chemical Engineering and Chemistry  
University of Washington  
Seattle, WA 98195 (USA)

[\*\*] This work has been supported in part by an AFOSR-MURI grant on smart-skin materials awarded to the University of Washington, and a research fellowship (awarded to Y. X.) from the David and Lucile Packard Foundation. Y. X. is a Camille Dreyfus Teacher Scholar and an Alfred P. Sloan Research Fellow.



**Scheme 1.** A schematic drawing of the spinneret constructed from two coaxial capillaries, and the molecular structures of MEH-PPV and PHT.

using syringe pumps. If no voltage was applied to the spinneret, orange MEH-PPV precipitate immediately appeared inside the PVP droplets at the orifice. When an appropriate voltage was applied, a stable compound jet could be formed, and fibers consisting of an MEH-PPV/PVP composite were generated as a result of stretching of the electrified jet via electrostatic forces. The spinning and stretching process was so fast that macroscopic precipitates were not observed in this process. Note that all the MEH-PPV solutions used in our experiments could not be electrospun as fibrous structures in the absence of the PVP solution. Figure 1A shows a fluorescence optical microscopy image of the as-spun nanofibers, clearly indicating that MEH-PPV had been homogeneously incorporated into the PVP nanofibers. After PVP had been

removed by ethanol extraction, fibrous structures with homogeneous fluorescence emission, characteristic of MEH-PPV, remained (Fig. 1B). Figure 1C shows a scanning electron microscopy (SEM) image of the as-spun MEH-PPV/PVP fibers with diameters in the range of 150–500 nm. As shown in the inset of Figure 1C, these fibers were featureless. Compared with pure PVP nanofibers electrospun from the same solution, the sample of composite fibers contained some beads  $\sim 1 \mu\text{m}$  in size. This observation suggests that the introduction of a MEH-PPV solution into the electrified jet might have slightly changed the viscoelastic behavior of PVP solution, and thus increased the instability of the jet. Nevertheless, all the beads disappeared after extraction with ethanol (Fig. 1D), suggesting that these beads were composed mainly of PVP. The higher-magnification SEM image (Fig. 1D, inset) indicates that the resultant fibers of MEH-PPV exhibit a ribbon-like structure with wrinkled surfaces and a thickness on the scale of  $\sim 30 \text{ nm}$ .

Ribbon-like fibers with wrinkled surfaces have also been observed in the electrospinning of MEH-PPV and other organic polymers.<sup>[18,20]</sup> The ribbon-like shape was usually attributed to the formation of a thin skin on the surface of a liquid jet in the early stage of electrospinning due to the rapid evaporation of solvent. As the solvent trapped inside the skin was removed in the later stage, a hollow structure was formed, which then collapsed under atmospheric pressure to form a ribbon.<sup>[20a]</sup> It is believed that the formation of the MEH-PPV ribbons shown in Figure 1D might involve a slightly different mechanism. As shown in the inset of Figure 1C, the as-spun MEH-PPV/PVP-blend fibers are characterized by uniformly circular cross-sections and very smooth surfaces. Transmission electron microscopy (TEM) studies (not shown here) indicated that the interiors of these fibers were densely filled with polymer. Based on these observations, we speculate that a triple-layered structure was formed in the as-spun fiber, with the core being relatively thin and made purely of MEH-PPV, and the outer shell being composed mainly of PVP. The middle shell between the core and the outer shell should contain a mixture of MEH-PPV and PVP due to the rapid evaporation of chloroform (the solvent used for the inner solution) and to the lateral diffusion between the inner and outer solutions during the electrospinning process.<sup>[15a]</sup> This picture is consistent with our recent report, where we demonstrated that the evaporation and diffusion of the solvents could drive the two polymers to mix together if two polymer solutions containing miscible solvents were electrospun through the two-capillary system.<sup>[15a]</sup> For this reason, we believe that our MEH-PPV/PVP fibers do not have a core–sheath structure with a clearly defined compositional profile as Sun et al. and Yu et al. have observed in their polymer systems.<sup>[15c,f]</sup> Nevertheless, when the PVP component was extracted from the as-spun fibers, the outer, featureless shells consisting mainly of PVP disappeared, and the middle shells shrank in volume and collapsed onto the cores to form ribbon-like structures with wrinkled surfaces.

The morphology and diameter of the resultant MEH-PPV fibers could be controlled by adjusting the concentration of

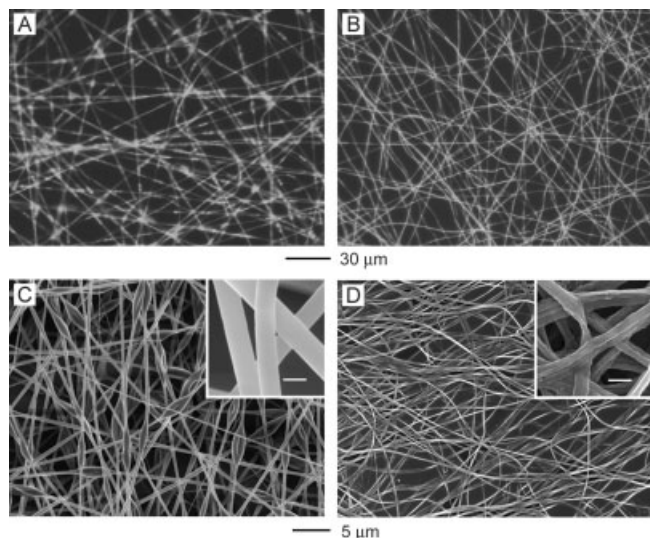


**Figure 1.** Fluorescence microscopy images of A) as-spun MEH-PPV/PVP fibers and B) pure MEH-PPV fibers fabricated by co-electrospinning an ethanol/water solution of PVP and a chloroform solution of MEH-PPV ( $3 \text{ mg mL}^{-1}$ ) through a two-capillary spinneret, followed by extraction of the PVP with ethanol. SEM images of C) the as-spun MEH-PPV/PVP fibers and D) the pure MEH-PPV fibers. The scale bars in the insets are 200 nm. These samples were prepared with a feed rate of MEH-PPV solution of  $0.3 \text{ mL h}^{-1}$ .

MEH-PPV solution and its feed rate. The fibers shown in Figure 1 were obtained from a solution containing  $3 \text{ mg mL}^{-1}$  MEH-PPV spun at a feed rate of  $0.3 \text{ mL h}^{-1}$ . The width of the MEH-PPV ribbons was around  $200 \text{ nm}$ . Increasing the concentration of MEH-PPV to  $5 \text{ mg mL}^{-1}$  led to the formation of ribbons up to  $350 \text{ nm}$  in width (Fig. 2A). When the concentration of MEH-PPV was reduced to  $1 \text{ mg mL}^{-1}$ , the resulting fibers became round in cross-section with a mean diameter around  $50 \text{ nm}$  (Fig. 2B). Small fibers (Fig. 2C) could also be obtained by reducing the feed rate of the MEH-PPV solution. In preparing the samples shown in Figures 2B,C, the feed rate of MEH-PPV was set at  $0.3 \text{ mg h}^{-1}$ . Since the concentration of MEH-PPV used in Figure 2B was three times less than that used in Figure 2C, the amount of ejected solvent was different

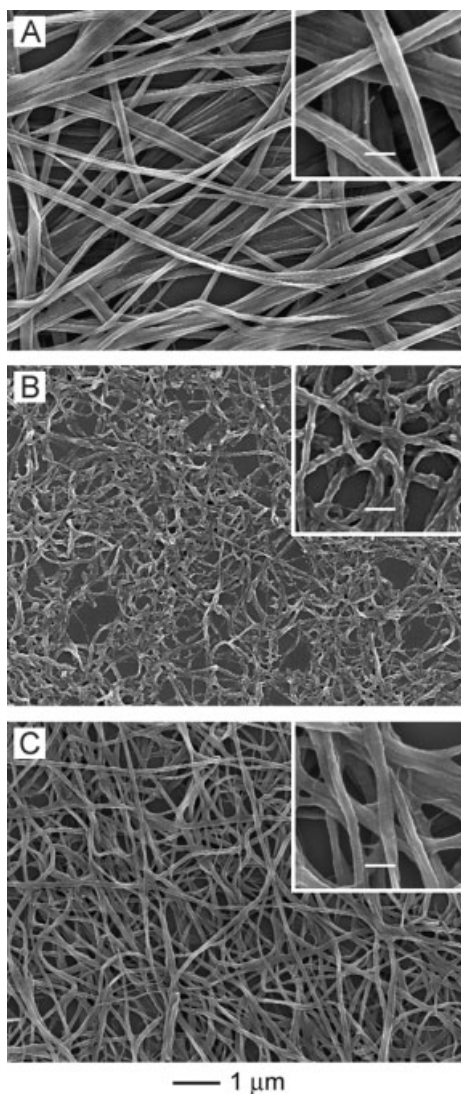


**Figure 2.** SEM images of MEH-PPV nanofibers electrospun from solutions containing different concentrations of MEH-PPV and at different feed rates: A) MEH-PPV:  $5 \text{ mg mL}^{-1}$ , feed rate:  $0.3 \text{ mL h}^{-1}$ ; B)  $1 \text{ mg mL}^{-1}$ ,  $0.3 \text{ mL h}^{-1}$ ; and C)  $3 \text{ mg mL}^{-1}$ ,  $0.1 \text{ mL h}^{-1}$ . The PVP component has been removed by ethanol extraction for all samples. The scale bars in the insets are  $200 \text{ nm}$ .

in these two cases. Although no considerable difference was observed in the MEH-PPV/PVP composite fibers, the resultant MEH-PPV fibers exhibited some differences in morphology. When a more dilute solution was used (Fig. 2B), the MEH-PPV fibers were more curved and tended to have circular cross-sections. This result could be attributed to a solvent-induced mixing effect: more solvent in the MEH-PPV solution might cause MEH-PPV to become better dispersed in the PVP matrix. As PVP was removed by solvent extraction, the MEH-PPV fibers experienced more shrinkage in the case of the more dilute solutions (Fig. 2B), forcing the fibers to become more deformed and distorted. All these results indicate that MEH-PPV and PVP were mixed in the as-spun fibers, and the extent of mixing was dependent on the volume of solvent contained in the compound jet.

We have also demonstrated the fabrication of nanofibers of MEH-PPV blended with other conjugated polymers. With the same setup, we simply used a blend solution of MEH-PPV and poly(3-hexylthiophene) (PHT) for electrospinning. In the case of conjugated polymers, formation of blends represents one of the simplest and most effective means for tuning their electronic and optoelectronic properties.<sup>[21,22]</sup> For example, blending can lead to various novel phenomena such as enhanced electroluminescence, photoinduced charge transfer, ambipolar charge transport, and lasing.<sup>[22]</sup> Figures 3A,B show typical SEM images of some MEH-PPV/PHT-blend fibers containing different amounts of PHT (PVP had already been

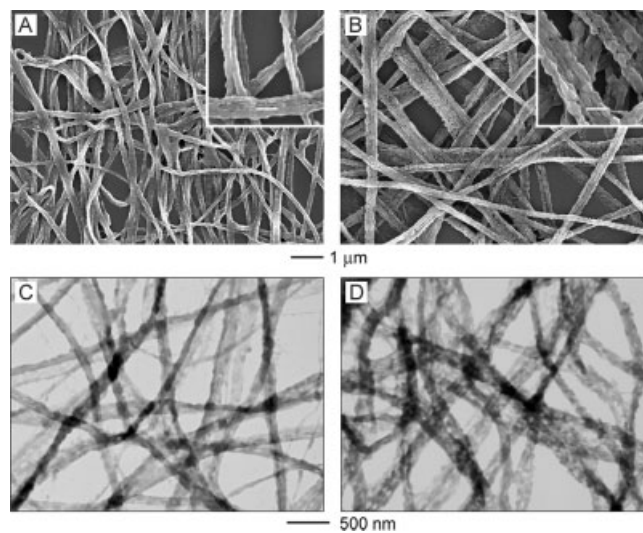


**Figure 3.** A,B) SEM and C,D) TEM images of MEH-PPV/PHT-blend nanofibers with different PHT contents. The PVP phase was removed by ethanol extraction for both samples. The PHT content is 30 wt.-% for the fibers in (A,C), and 80 wt.-% for the fibers in (B,D). The scale bars in the insets are  $200 \text{ nm}$ .

removed by ethanol extraction). The presence of PHT in these products was confirmed by energy-dispersive X-ray (EDX) analysis. Compared to pure MEH-PPV fibers, the surfaces of these blend fibers were much rougher. It can be seen

that these fibers are composed mainly of small particles with dimensions in the range of 30 to 50 nm. As evidenced by TEM studies (Figs. 3C,D), these nanoparticles could be assigned as PHT since the PHT phase exhibited a higher contrast in TEM due to the presence of sulfur. The TEM images also established that these two components were phase-separated within the fibers. However, the mean domain size of the PHT phase was much smaller than those of the MEH-PPV/PHT-blend films prepared by spin-casting (where the domain sizes were on the order of 100–150 nm). Rapid solidification associated with an electrospinning process might have inhibited the large-scale phase separation in the electrospun fibers. A reduction in phase separation was also supported by their optical properties, discussed below.

Figure 4 shows the absorption and photoluminescence (PL) emission spectra obtained from spin-cast thin films and non-woven mats of the electrospun nanofibers. For both MEH-

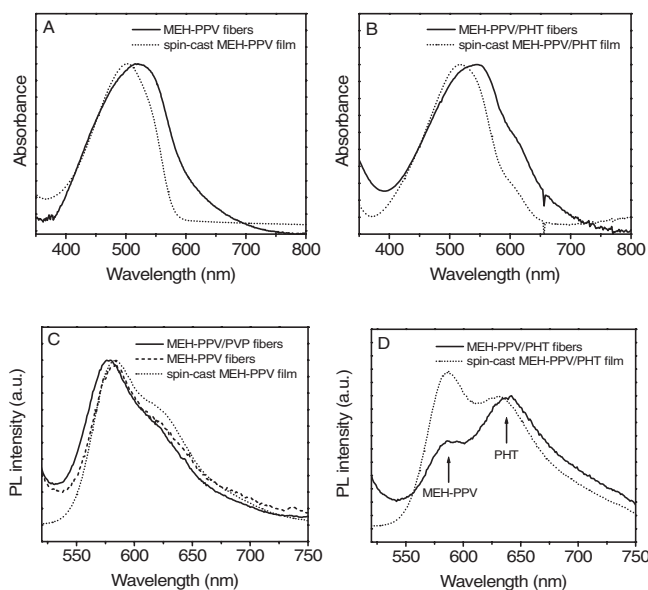


**Figure 4.** A,B) Absorption and C,D) PL spectra obtained from MEH-PPV nanofibers or spin-coated thin films (A,C) and MEH-PPV/PHT-blend nanofibers or spin-cast thin films containing 30 wt.-% PHT (B,D).

PPV and the MEH-PPV/PHT blend, the absorption peak of electrospun nanofibers is slightly red-shifted compared to the thin films (Figs. 4A,B). In addition, the absorption band of the nanofibers is broadened suggesting a more inhomogeneous environment, as reported for MEH-PPV in aligned mesoporous silica.<sup>[13b]</sup> The red-shift in the absorption peak implies that there is a change in chain distribution within each nanofiber towards a more extended conformation and better delocalized  $\pi$ -conjugation.<sup>[13b,23]</sup> We believe that this conjugation length increase is a result of the significant stretching of the liquid jet during the electrospinning process. Such an effect has also been observed in mechanically stretched films of MEH-PPV/polyethylene blends.<sup>[24]</sup>

Unlike the absorption spectra, the PL emission spectrum of the pure MEH-PPV nanofibers is very similar to that of a spin-cast thin film (Fig. 4C). In this case, the as-spun MEH-PPV/PVP composite fibers exhibited a slightly blue-shifted emission due to the insulating nature of remaining PVP in the fibers. The emission spectra recorded from the MEH-PPV/PHT-blend nanofibers showed some interesting features. The spectra were composed of contributions from both MEH-PPV (580 nm) and PHT (640 nm). Figure 4D shows the emission spectra of 30 wt.-% PHT-blend nanofibers and the related spin-cast thin film. It can be seen that the emission band near 580 nm (corresponding to the MEH-PPV component in the electrospun fibers) is much weaker than that of the spin-cast films. Similar quenching of the MEH-PPV emission was also observed in nanofibers with other compositions. The enhanced quenching efficiency for the MEH-PPV emission in the nanofibers clearly indicates a more efficient energy-transfer process from MEH-PPV to PHT due to the stronger interaction between MEH-PPV and PHT in these confined nanostructures, as compared to the bulk thin films.

In summary, we have demonstrated that nanofibers of conjugated polymers and their blends could be conveniently fabricated by co-electrospinning their solutions with a spinnable matrix polymer solution, followed by extraction of the matrix polymer. The morphology and diameters of the resulting fibers could be controlled by adjusting the processing parameters. Compared with spin-cast films, the polymer chains in electrospun fibers seemed to have a more extended conformation and better spatial orientation. In particular, we have demonstrated that the length scale of phase separation involved in electrospun fibers of polymer blends could be greatly reduced, leading to more efficient energy transfer between the blend components in the confined 1D systems. Our results clearly establish that electrospinning is not only a simple method of generating ultrathin conjugated-polymer fibers, but also an effective means for tuning the microstructures and properties. Although the present work has been mainly focused on MEH-PPV, we believe that the method described here could be extended to provide a generic route to the preparation of nanofibers from other polymers that cannot be directly electrospun using the conventional single-capillary setup. Furthermore, our work demonstrates that two polymer solutions that are not mixable in a conventional fashion may be mixed at the nanometer-length scale through the use of a simple co-spinning scheme to generate uniform and homogeneous composite nanofibers.

### Experimental

The spinneret consisting of two coaxial capillaries was fabricated according to our previously reported procedure [15a]. As shown in Scheme 1, a polyimide-coated silica capillary was guided to penetrate the wall of a plastic syringe, and then inserted into a stainless steel needle. In a typical procedure for electrospinning, a solution containing 0.6 g poly(vinyl pyrrolidone) (PVP) (Aldrich, weight-average molecular weight  $M_w \approx 1\,300\,000$ ), 1.5 mL water, and 8.5 mL ethanol

was added to the syringe connected to the metallic needle, and a poly[2-methoxy-5-(2-ethylhexyloxy)-1,4-phenylenevinylene] (MEH-PPV) ( $M_w \approx 1\,000\,000$ , American Dye Source) solution in chloroform was added to another syringe connected to the silica capillary. The two solutions were fed into the capillaries by two syringe pumps (KDS-200, Stoelting, Wood Dale, IL). The feed rate for the PVP solution was set at  $0.6\text{ mL h}^{-1}$ . The feed rate for the MEH-PPV solution was varied in the range of  $0.05\text{--}0.3\text{ mL h}^{-1}$ . The metallic needle was connected to a high-voltage power supply (ES30P-5W, Gamma High Voltage Research, FL), and a piece of aluminum foil or a silicon wafer (Silicon Sense, Nashua, NH) was placed 9 cm below the tip of the needle to collect the nanofibers. The spinning voltage was set at 7.5 kV. PVP was extracted by immersing the as-spun fibers in ethanol for 2 h. The samples were then dried overnight at  $60^\circ\text{C}$  in a vacuum oven. In preparing the MEH-PPV/PHT-blend fibers, a certain amount of poly(3-hexylthiophene) (PHT) ( $M_w \approx 19\,400$ , Aldrich) was added to the MEH-PPV solution. The concentration of MEH-PPV was fixed at  $2.5\text{ mg mL}^{-1}$ , while the amount of PHT was varied from 30 to 80 wt.-%. Fluorescent images of as-spun fibers were taken using a Leica optical microscope (DMIRBE, Leica Microsystems, Bannockburn, IL). Scanning electron microscopy (SEM) images were acquired using a field-emission microscope (Sirion, FEI, Hillsboro, OR) operated at an accelerating voltage of 5 kV. Before imaging, a thin layer of Au/Pd ( $\sim 5\text{ nm}$  thick) was sputtered onto the samples. Energy-dispersive X-ray (EDX) measurements were conducted with an EDAX system (Mahwah, NJ) attached to the same microscope, but with no Au/Pd coating for the samples. Transmission electron microscopy (TEM) images were acquired using a Philips EM-430 microscope operated at 80 kV. Optical absorption spectra were obtained using a Cary 5E (Varian, Walnut Creek, CA) spectrometer. Steady-state photoluminescence (PL) spectra were recorded on a PTI QM-2001-4 (Lawrenceville, NJ) spectrophotometer with an excitation wavelength of 500 nm.

Received: April 22, 2004

Final version: July 16, 2004

Published online: October 20, 2004

- [1] See recent reviews: a) D. H. Reneker, I. Chun, *Nanotechnology* **1996**, 7, 216. b) A. Frenot, I. S. Chronakis, *Curr. Opin. Colloid Interface Sci.* **2003**, 8, 64. c) D. Li, Y. Xia, *Adv. Mater.* **2004**, 16, 1151.
- [2] See examples: a) G. Srinivasan, D. H. Reneker, *Polym. Int.* **1995**, 36, 195. b) K. Ohgo, C. Zhao, M. Kobayashi, T. Asakura, *Polymer* **2003**, 44, 841. c) A. G. MacDiarmid, W. E. Jones, I. D. Norris, J. Gao, A. T. Johnson, N. J. Pinto, J. Hone, B. Han, F. K. Ko, H. Okuzaki, M. Llaguno, *Synth. Met.* **2001**, 119, 27. d) H. Fong, D. H. Reneker, *J. Polym. Sci., Part A: Polym. Chem.* **1999**, 37, 3488. e) H.-J. Jin, S. V. Fridrikh, G. C. Rutledge, D. L. Kaplan, *Biomacromolecules* **2002**, 3, 1233. f) M. Bognitzki, W. Czado, T. Frese, A. Schaper, M. Hellwig, M. Steinhart, A. Greiner, J. H. Wendorff, *Adv. Mater.* **2001**, 13, 70.
- [3] a) W.-J. Li, C. T. Laurencin, E. J. Caterson, R. S. Tuan, F. K. Ko, *J. Biomed. Mater. Res.* **2002**, 60, 613. b) Y. Yoshimoto, Y. M. Shin, H. Terai, J. P. Vacanti, *Biomaterials* **2003**, 24, 2077. c) X. M. Mo, C. Y. Xu, M. Kotaki, S. Ramakrishna, *Biomaterials* **2004**, 25, 1883. d) J. Chen, V. Karageorgiou, G. H. Altman, D. L. Kaplan, *Biomaterials* **2004**, 25, 1039.
- [4] a) H. Jia, G. Zhu, B. Vugrinovich, W. Kataphinan, D. H. Reneker, P. Wang, *Biotechnol. Prog.* **2002**, 18, 1027. b) J. Xie, Y.-L. Hsieh, *J. Mater. Sci.* **2003**, 38, 2125. c) M. M. Demir, M. A. Gulgun, Y. Z. Menceloglu, B. Erman, S. S. Abramchuk, E. E. Makhaeva, A. R. Khokhlov, V. G. Matveeva, M. G. Sulman, *Macromolecules* **2004**, 37, 573.
- [5] X. Wang, C. Drew, S.-H. Lee, K. J. Senecal, J. Kumar, L. A. Samuelson, *Nano Lett.* **2002**, 2, 1273.
- [6] a) J.-S. Kim, D. H. Reneker, *Polym. Compos.* **1999**, 20, 124. b) M. M. Bergshoeff, G. J. Vancso, *Adv. Mater.* **1999**, 11, 1362.
- [7] C. Kim, K. S. Yang, *Appl. Phys. Lett.* **2003**, 83, 1216.
- [8] S. W. Choi, S. M. Jo, W. S. Lee, Y.-R. Kim, *Adv. Mater.* **2003**, 15, 2027.
- [9] a) D. Li, Y. Wang, Y. Xia, *Nano Lett.* **2003**, 3, 1167. b) D. Li, Y. Wang, Y. Xia, *Adv. Mater.* **2004**, 16, 361. c) A. Theron, E. Zussman, A. L. Yarin, *Nanotechnology* **2001**, 12, 384. d) E. Zussman, A. Theron, A. L. Yarin, *Appl. Phys. Lett.* **2003**, 82, 973.
- [10] a) D. H. Reneker, A. L. Yarin, H. Fong, S. Koombhongse, *J. Appl. Phys.* **2000**, 87, 4531. b) Y. M. Shin, M. M. Hohman, M. P. Brenner, G. C. Rutledge, *Appl. Phys. Lett.* **2001**, 78, 1149.
- [11] a) A. J. Heeger, *Angew. Chem. Int. Ed.* **2001**, 40, 2591. b) A. G. MacDiarmid, *Angew. Chem. Int. Ed.* **2001**, 40, 2581. c) *Handbook of Organic Conductive Molecules and Polymers* (Ed: H. S. Nalwa), Wiley, New York **1997**. d) A. Kraft, A. C. Grimsdale, A. B. Holmes, *Angew. Chem. Int. Ed.* **1998**, 37, 402.
- [12] a) R. Jaeger, H. Schönherr, G. J. Vancso, *Macromolecules* **1996**, 29, 7634. b) D. Y. Lin, D. C. Martin, *Polym. Prepr. (Am. Chem. Soc., Div. Polym. Chem.)* **2003**, 44, 70. c) A. Pedicini, R. J. Farris, *Polymer* **2003**, 44, 6857.
- [13] a) R. J. O. M. Hoofman, M. P. de Haas, L. D. A. Siebbeles, J. M. Warman, *Nature* **1998**, 392, 54. b) T.-Q. Nguyen, J. Wu, V. Doan, B. J. Schwartz, S. H. Tolbert, *Science* **2000**, 288, 652.
- [14] a) I. D. Norris, M. M. Shaker, F. K. Ko, A. G. MacDiarmid, *Synth. Met.* **2000**, 114, 109. b) K. Desai, C. Sung, *Mater. Res. Soc. Symp. Proc.* **2003**, 788, 209. c) P. K. Kahol, N. J. Pinto, *Synth. Met.* **2004**, 140, 269.
- [15] a) D. Li, Y. Xia, *Nano Lett.* **2004**, 4, 933. b) I. G. Loscertales, A. Barrero, M. Marquez, R. Spretz, R. Velarde-Ortiz, G. Larsen, *J. Am. Chem. Soc.* **2004**, 126, 5376. c) I. G. Loscertales, A. Barrero, I. Guerrero, R. Cortijo, M. Marquez, A. M. Ganán-Calvo, *Science* **2002**, 295, 1695. d) J. M. Lopez-Herrera, A. Lopez, A. Barrero, I. G. Loscertales, M. Marquez, *J. Aerosol Sci.* **2003**, 34, 535. e) Z. Sun, E. Zussman, A. L. Yarin, J. H. Wendorff, A. Greiner, *Adv. Mater.* **2003**, 15, 1929. f) J. H. Yu, S. V. Fridrikh, G. C. Rutledge, *Adv. Mater.* **2004**, 16, 1562.
- [16] a) D. Braun, A. J. Heeger, *Appl. Phys. Lett.* **1991**, 58, 1982. b) G. Yu, A. J. Heeger, *J. Appl. Phys.* **1995**, 78, 4510. c) S. A. Jenekhe, S. Yi, *Appl. Phys. Lett.* **2000**, 77, 2635. d) G. Yu, J. Gao, J. C. Hummelen, F. Wudl, A. J. Heeger, *Science* **1995**, 270, 1789. e) U. Scherf, S. Riechel, U. Lemmer, R. F. Mahrt, *Curr. Opin. Solid State Mater. Sci.* **2001**, 5, 143.
- [17] a) J. G. Park, G. T. Kim, J. H. Park, H. Y. Yu, G. McIntosh, V. Krstic, S. H. Jhang, B. Kim, S. H. Lee, S. W. Lee, M. Burghard, S. Roth, Y. W. Park, *Thin Solid Films* **2001**, 393, 161. b) A. Noy, A. E. Miller, J. E. Klare, B. L. Weeks, B. W. Woods, J. J. DeYoreo, *Nano Lett.* **2002**, 2, 109.
- [18] S. Madhugiri, A. Dalton, J. Gutierrez, J. P. Ferraris, K. J. Balkus, Jr., *J. Am. Chem. Soc.* **2003**, 125, 14531.
- [19] a) D. Li, Y. Xia, *Nano Lett.* **2003**, 3, 555. b) D. Li, T. Herricks, Y. Xia, *Appl. Phys. Lett.* **2003**, 83, 4586.
- [20] a) S. Koombhongse, W. Liu, D. H. Renek, *J. Polym. Sci., Part B: Polym. Phys.* **2001**, 39, 2598. b) H. Fong, W. Liu, C.-S. Wang, R. A. Vaia, *Polymer* **2002**, 43, 775. c) S. Megelski, J. S. Stephens, D. B. Chase, J. F. Rabolt, *Macromolecules* **2002**, 35, 8456.
- [21] a) M. Berggren, O. Inganäs, G. Gustafsson, J. Rasmussen, M. R. Andersson, T. Hjertberg, O. Wennerström, *Nature* **1994**, 372, 444. b) S. A. Jenekhe, J. A. Osaheni, *Science* **1994**, 265, 765. c) J. A. Osaheni, S. A. Jenekhe, *Macromolecules* **1994**, 27, 739.
- [22] a) G. Yu, H. Nishino, A. J. Heeger, T.-A. Chen, R. D. Rieke, *Synth. Met.* **1995**, 72, 249. b) X. L. Chen, S. A. Jenekhe, *Macromolecules* **1997**, 30, 1728. c) S. A. Jenekhe, L. R. de Paor, X. L. Chen, R. M. Tarkka, *Chem. Mater.* **1996**, 8, 2401. d) X. Zhang, D. M. Kale, S. A. Jenekhe, *Macromolecules* **2002**, 35, 382. e) A. Babel, J. D. Wind, S. A. Jenekhe, *Adv. Funct. Mater.* **2004**, 14, 891.
- [23] B. J. Schwartz, *Annu. Rev. Phys. Chem.* **2003**, 54, 141.
- [24] T. W. Hagler, K. Pakbaz, K. F. Voss, A. J. Heeger, *Phys. Rev. B: Condens. Matter Mater. Phys.* **1991**, 44, 8652.